Deterministic Modeling of Solidification Microstructure Formation in Directed Energy Deposition Fabricated Ti6Al4V

Jinghao Li, Xianglin Zhou, Qingbo Meng, Mathieu Brochu, Nejib Chekir, J Sixsmith, J Hascoët, Yaoyao Zhao

Deterministic Modeling of Solidification Microstructure Formation in Directed Energy Deposition Fabricated Ti6Al4V

Jinghao Li[1], Xianglin Zhou[2,] *, Qingbo Meng[2], Mathieu Brochu[3], Nejib Chekir[3,4], J.J. Sixsmith[4], J.Y. Hascoët[5], Yaoyao Fiona Zhao[1,] *

[1]Department of Mechanical Engineering, McGill University, Montreal, Québec, Canada H2A 0C3; [2]State Key Laboratory for Advance Metals and Materials, University of Science and Technology, Beijing, China 10083; [3]Department of Mining and Materials Engineering, McGill University, Montreal, Québec, Canada H3A 2B2; [4]Liburdi Automation Inc., Dundas, Ontario, Canada L9H 7K4; [5]Institut de Recherche en Génie Civil et Mécanique (GeM), UMR CNRS 6183 Ecole Centrale de Nantes, Nantes, France, 44321

Abstract

Metal additive manufacturing (MAM) technology is now widely applied in the manufacturing and remanufacturing industry, among which microstructure simulation gradually shows its importance. Traditional solidification microstructure simulation methods all have their merits as well as drawbacks when applied in MAM cases. In this work, a deterministic solidification microstructure model, named "invasion model", is established to avoid the essential defects of traditional methods. This model focuses on the interaction between the neighboring bi-crystals instead of simulating the growth kinetics of each columnar grain or deriving the field form of variables. Within a bi-crystal system, the grain boundary tilt from thermal gradient direction is understood as a transient invasion behavior of one grain to another, and the competitive grain growth behavior along the buildup process of MAM is a summary of all the invasions in bi-crystal systems. To fill the gaps in the rapid solidification theory, a database recording the anisotropic growth effect under a rapid directional solidification condition was established with the help of an artificial neural network (ANN). Wire feed directed energy deposition (DED) fabricated Ti6Al4V thin-wall samples with full dendritic columnar grains (prior beta) are used as a benchmark to test the validation of the novel simulation model. The grain geometrical structure of reconstructed prior β grains along the build-up direction has a good agreement with the simulation result. The model can also be applied to other cases of MAM or combine with various models to achieve real-time as-solidified crystallographic feature prediction when it meets the scope of application.

Keywords: Additive Manufacturing; Microstructure; Modeling; Solidification

1 Introduction

Metal additive manufacturing (MAM) technology is now changing the pattern of the high-end manufacturing industry, among which MAM fabricated Ti6Al4V has been by far the most extensively investigated material and attracts a lot of research interests. MAM has a unique ability to create complex components, such as hollow and complex curved surfaces that may otherwise be impossible to other manufacturing methods. However, uncertainties in MAM such as chemical composition, microstructure, texture, and mechanical properties are restricting its development and application. Recognizing the interplay between material deposition phenomena and process factors in AM is crucial for component quality control. Modeling approaches and numerical simulations on multiple length scales and timescales are the ideal tools to save time

and experimental costs. These models enable mechanical property predictions from the process and material parameters and serve as a guideline for further property optimization.

Microstructure simulation for MAM is blooming recently as a result of the rapid development of MAM techniques and microstructure simulation methods. Now, there are three methods widely applied to achieve the solidification microstructure simulation for MAM, namely cellular automata (CA), phase-field (PF), and kinetic Monte Carlo (KMC). Among these three methods, CA is the first commercialized method because it is capable to provide the microstructure information in meso- and macro-scale where many practical significances can be found. It has already been used for the MAM cases at a three-dimensional (3D) level by combining the thermal history data from macroscale transform phenomenon simulations, such as finite element analysis (FEA), finite difference, or Lattice Boltzmann methods. However, CA models are established based on tip kinetics which typically assumes local equilibrium or a quasi-stationary condition, and it is not appropriate under rapid cooling conditions in MAM. The PF method is the most accurate method amongst the three. It is capable to capture sub-grain features such as secondary or higher-order dendrites [1-3]. However, the PF method works on a very small time and space scale due to physics. The application of the PF method at 3D level and large scale renders the level of computational resources required prohibitive. As for the KMC method, the crystal orientations are often neglected in this method resulting in the simulated grains structure to be less accurate due to the weak physical background [4]. The models based on these three existing simulation methods have limited practical significance for the cases in MAM: either the simulation domain cannot reach a part-level scale, or the physical background is not found enough for a quantitively analysis of the solidification microstructure evolution. Thus, the comparison between the microstructure simulation and experimental result are mostly carried out on texture and statistical results [4, 5].

Competitive grain growth behavior has been intensively studied for the nickel-based single crystal materials in directional solidification. However, a limited number of studies have been carried out for MAM techniques because of the complex solidification condition with multiple phases and fields involved. Furthermore, the gaps in rapid solidification theories left many physical parameters unquantified which is still a difficulty in traditional solidification microstructure simulation methods. Another problem is the treatment of the nucleation and crystal orientations which are usually set as random factors. This also renders the simulated grain structure to be quantitative. A very good work conducted by Pineau *et al.* [6] shows that even for a simple case of bi-crystal under directional solidification, the computed grain boundary orientation map shows dramatic differences between CA and PF models, let alone the complex solidification conditions in MAM. This can be attributed to the differences in the methodology between CA and PF, as well as the assumptions made in these two types of models.

MAM techniques usually build a part in a layer-by-layer fashion. This also means the previously deposited material becomes the substrate of the next. From a microstructural point of view, the previously deposited microstructure has a profound influence on the subsequent portion as the newly deposited material tends to inherit the existing crystallographic features from the preceding layer, like crystal orientations and grain boundaries. This phenomenon is called “epitaxial grain growth”. Instead of creating a new crystal, the fusion near liquidus tends to solidify and nucleates on the surface of half-melted grains to save free energy. Thus, in most of the MAM cases, the crystal geometrical structure is frequently found to be in a columnar manner and the columnar grains can go through multiple layers in deposition processes. These anisotropic columnar grain structures have a great influence on the mechanical properties of the

printed part as they lose their effect of cleavage-cracking resistance [7] in the build-up direction. Even though great efforts have been made to achieve the columnar to equiaxed transition (CET) for different alloy systems, accurate modeling of these columnar grains is still indispensable as it could provide a guideline on process parameter control when the achievement of CET is very difficult or even not possible. MAM techniques enable a more accurate real-time local solidification condition control. However, until now, a practical way to quantitively simulate the development of the columnar grains in MAM is basically nonexistent. Especially, for the DED fabricated Ti6Al4V, columnar grains can develop into millimeter-scale and grain number is countable. Therefore, a deterministic model describing the microstructure quantitatively instead of statistically shows its importance compared to the probabilistic models such as CA and KMC.
To accurately control and optimize of the microstructure in MAM, a novel model named "invasion model" is proposed in this research to quantitively investigate the competitive grain growth behavior under complex solidification conditions. This model focuses on the quantitative analysis of the grain boundary tilt angle between the bi-crystal systems during the solidification process. It believes the grain boundary of a bi-crystal system in a compressed mushy zone tilts from the thermal gradient direction because of two effects: anisotropic growth and Marangoni convection. The grain boundary angle with regard to the thermal gradient direction is considered as a crystal invading its adjacent crystal, hence the term "invasion model" is named. In this study, wire DED fabricated Ti6Al4V is selected as a benchmark to validate the model considering the assumptions made. By combining the grain boundary behaviors in bi-crystal systems, solidification microstructure evolution is simulated during the materials deposition process and shows a good agreement with the experimental result. This model can also be adapted for other cases in MAM for different single-phase alloy systems under a part scale where more practical significance can be found. Furthermore, the databases built during this strategy have great significance either to conduct other grain growth studies or to validate the existing simulation models.

2. Physical Background

Solidification is never an easy problem since it involves the phenomena of the interface movement and multiple phase transformation. Solidification condition of MAM within a melt pool is a more complex case than casting as the solidification interface in a melt pool is a small, highly nonlinear free-form interface. In MAM, solidification usually takes place under a rapid and steep thermal gradient condition where various physical parameters are difficult or even impossible to be quantified. The highly nonlinear interface evolution during the solidification process in most cases becomes the biggest problem for solidification microstructure simulation techniques. To describe the microscale features of material microstructure, simulation techniques need to mesh up the investigated domain in an even finer manner, which is typically recommended to be ten times finer than the feature scale to stabilize the simulation result. It leads to a requirement of enormous computational power making it impossible for a part level solidification microstructure simulation.
Considering the nature of a constrained epitaxial grain growth under a steep thermal gradient condition, the ambient environment of a bi-crystal solidification in MAM is shown in Figure 1. The two grains within a bi-crystal system are depicted with different colors with the grids representing their crystal orientations, respectively. The solute concentration field is schematically shown above the liquidus line which can be influenced by the movement of the

fusion driven by the Marangoni effect. The large thermal gradient value generated from MAM processes compresses the mushy zone of solidification at the melt pool bottom into a very thin film. Based on the knowledge of welding for reference [8], the primary arm spacing under different cooling condition is described by:

$$\lambda_1 = a(G^2R)^{-1/4} \quad (1)$$

Where λ_1 refers to the primary arm spacing, a is the material-dependent coefficient, G is thermal gradient and R is solidification rate. In the case of MAM, λ_1 usually becomes very small with large $G\&R$ because of the negative correlation embodied in equation (1).

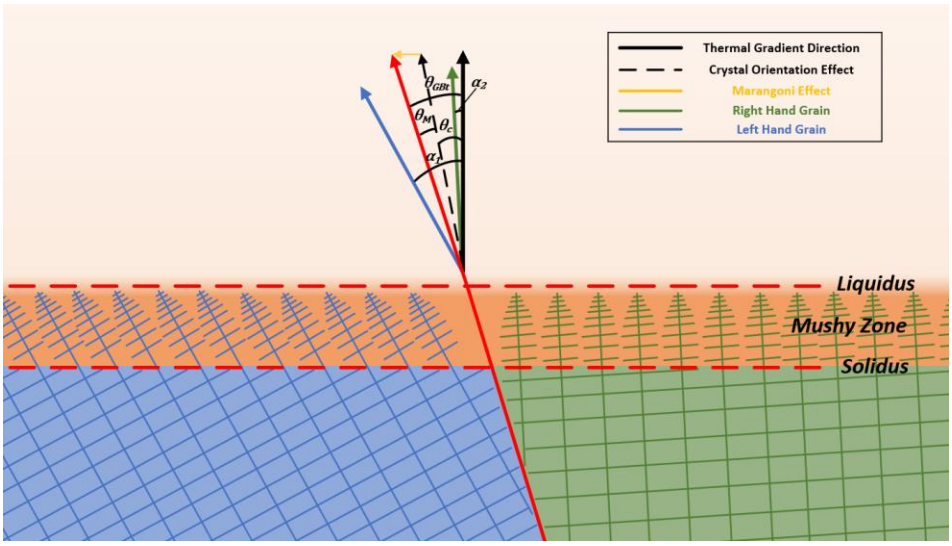

Figure 1: Local solidification condition for a bi-crystal system in MAM.

Under the condition of rapid solidification in the DED process, the primary spacing of dendritic grains are very small, and they are paratactic within a single columnar grain domain as a result of epitaxial grain growth. In the case of DED fabricated Ti6Al4V, the original solidification microstructural features are eliminated by the solid-phase transformation. However, evidence can be found in the simulation studies showing that the primary dendritic grains have a periodic behavior occupying its neighboring grains [9]. With a proper selection of the length scale, this periodic behavior can be showed as a straight line as the waving curves generated at the grain boundary is usually less important when grain selection and grain size change are investigated at part-scale.

As for how a grain boundary is developed between a bi-crystal system under the MAM solidification condition, a hypothetical situation is first assumed where crystal orientations within a bi-crystal system are perfectly symmetrical. The total supercooling ΔT, which is the driving force of solidification front development, can be attributed to the sum of four contributions:

$$\Delta T = \Delta T_{th} + \Delta T_c + \Delta T_k + \Delta T_r \quad (2)$$

where ΔT_{th} is the pure thermal undercooling at solid/liquid interface caused by thermal diffusion, ΔT_c stands for the undercooling contributions associated with solute diffusion, ΔT_k is the kinetic supercooling influenced by the rate at which atoms attach to the solid phase, ΔT_r is the curvature supercooling due to curvature of the solid-liquid interface, also called Gibbs-Thomson supercooling. Based on the symmetry principle of the hypothetical situation, ΔT_{th}, ΔT_k and ΔT_c

on the right-hand side of equation (2) are not able to make the grain boundary tilt from the initial normal direction of the solidification front. The three contributions all make the grain growth normal to the original liquidus line, which means the column grains (cluster of small dendritic columnar grain with same crystal orientations) are always perfectly parallel with each other if the solidification front is stable. However, for the solidification of metal alloys, the Marangoni effect influences the solute concentration in fusion and leads to different constitutional supercooling (ΔT_c) that breaks the symmetry of the system. In the case of DED fabricated Ti6Al4V, the surface tension-temperature coefficient is negative and the fusion from the laser exposure area with higher temperature tends to flow toward the boundary of the melt pool. And the flow direction near the mushy zone driven by the Marangoni effect has important implications for the grain growth direction as well as the development direction of grain boundaries in the solidification process of metal alloys.

In another solidification case of the bi-crystal system, if the two grains with different crystal orientations are solidified under the directional solidification condition (constant isotherm normal to solidification direction and without flow velocity at solidification front), the crystal orientation relation decides the grain boundary development direction, also called anisotropic growth effect. In general, the crystals with preferred crystal orientation (e.g. one of <001> directions in cubic crystals go most closely aligned with the normal direction of solidification front) have the advantage to win the competitive grain growth. This phenomenon is widely found in metallic alloy materials under the directional solidification experiments, the grain boundaries are found to tilt from the normal direction of the solidification front because of the different crystal orientation relations among the adjacent grains [10]. Between these two extremes, conditions of solidification microstructure development in MAM are usually a combination of the two cases and some key physical realities and phenomena are detailly described below. In this work, dendritic columnar grains are referred to as column grains or grains for simplicity, and angles in a two-dimensional (2D) model are defined as negative in a clockwise direction and positive in counterclockwise.

2.1 Dendritic Columnar grains

The columnar dendritic growth is characterized by the constrained growth of a packet of dendrites along the same general direction. Studies have shown that the columnar grain is a universal phenomenon in solidification microstructure not limited to DED but most of MAM technologies [4]. This can be addressed to the cooling condition at the melt pool bottoms in terms of the thermal gradient (G) and solidification rate (R) as the solidification conditions of DED technology are mostly located at the columnar grain area of the G-R diagram. In DED fabricated Ti6Al4V, the column grains as well as grain boundaries tend to elongate along the built direction penetrating multiple layers but they do not always strictly follow the thermal gradient direction. Based on experimental observation, the grain boundaries can maintain a straight line in a long-range between the same bi-crystal system under a relatively constant cooling condition (stable melt pool geometry). This is the base indicating that the grain boundary tilting and grain size change can be modeled quantitatively.

A finer microstructure is usually desired in material science to achieve a better mechanical property according to the famous Hall-Patch relationship and as a result of cleavage cracking resistance effect. Thus, a great amount of work focuses on achieving the CET for different materials in MAM [11, 12]. This can be accomplished by the process parameter control, process

optimization, promoting nucleation, and so on. From the modeling point of view, if fully equiaxial grain structures are achieved, the average grain size or the grain size change is usually of more importance which is determined by the maximum nucleation number (n_{max}, usually measured from the experimental result) arranged in the simulation domain. A simple Voronoi diagram is a good representation of the equiaxial solidification microstructure with a random nucleation position and crystal orientation assumption. However, for some types of material, the process parameter is only achieved in a certain range to get a successful print without defects like cracks or porosity. In this case, the columnar grains are inevitably produced. For DED fabricated Ti6Al4V, constitutional supercooling cannot achieve the amount requested for nucleation and there is no refiner for this type of material. The columnar grains can then grow into several millimeters thick penetrating hundreds of deposition layers, therefore, accurate modeling and controlling of the columnar grain structures becomes important.

2.2 Nucleation and epitaxial grain growth

According to the independent nucleation theory [12], Ti6Al4V is a material that has inadequate constitutional supercooling for nucleation. Thus, in most cases of DED fabricated Ti6Al4V parts, the added material epitaxially grows from the existing half-melt crystals to save free energy instead of creating a new nucleus. This was also approved by the experimental observation that only a limited number of new crystals with random crystal orientations generate along the material deposition process. In the wire DED Ti6Al4V fabrication studied in this work, the nucleation rule is set based on the "no nucleation assumption". This assumption believes there are all epitaxial grain growth and no grains with new crystal orientation are introduced in the simulation domain during the material deposition process. However, this assumption is not suitable for cases like selective laser melting (SLM) and DED processed Ti6Al4V with powder feedstock, as the unmelt powders or external material inevitably become the substrate for epitaxial grain growth and introduce grains with new crystal orientation into the printed zone. In this case, the random crystal orientation rule should be set as a boundary condition to investigate the competitive grain growth as it is almost impossible to measure the exact crystal orientations as boundary conditions for simulation.

For materials that CET can be achieved during the MAM processes, traditional nucleation rules (e.g. continuous nucleation) should be applied which arranges nucleation numbers according to the density of grains in each time step with random crystal orientations. Due to the remelting effect of MAM techniques, even the CET can be achieved within the melt pool, it is still possible that remelting eliminates the equiaxial grain area (typically located at the top area of a melt pool), and the columnar grain dominates the printing area. In this case, the competitive grain growth can still be analyzed quantitively under no nucleation assumption.

2.3 Preferred grain growth direction and grain selection mechanism

Starting from the research conducted by Walton and Chalmers [13], people recognized that metallic materials have their preferred grain growth directions (<100> of cubic crystal systems and <1010> for hexagonal closed pack). This means on the preferred grain growth directions there is a higher grain growth velocity compared to other directions. This is a result of anisotropic surface energy in different packing manner of metal atoms. According to crystallographic symmetry, <001> directions are 90 degrees apart in body-center cubic (bcc) and face-center cubic (fcc) crystals which is also referred to as four-fold symmetry. Under a 2D bi-crystal system, the grain selection mechanism is intensively investigated and there are two

situations namely diverging and converging based on crystal orientation relations. In general, the grains with their preferred grain growth directions align with the solidification front (favorably oriented grains) have the advantage to win the competitive grain growth. Under a converging situation of a bi-crystal system, the unpreferred grain needs a higher supercooling to catch up with the solidification front compared to the preferred one. The small lag caused by this phenomenon makes the unpreferred grain hit the side of the preferred one and results in a grain boundary perfectly align with the <01> direction of the preferred one. If the two grains in a bi-crystal system are diverging, secondary and higher-order dendrites can develop into the open region and generates a grain boundary within the angle between the <01> directions of the two grains. Following this, the most famous grain selection mechanism is called best align criterion with the following formula:

$$\theta_{GB} = \begin{cases} \alpha_1 \; if \; |\alpha_1| < |\alpha_2| \\ \alpha_2 \; if \; |\alpha_2| < |\alpha_1| \end{cases} \tag{3}$$

In the best align grain selection mechanism, three criteria are followed according to the symmetric principle in its selection map: 1. the value of the grain boundary angle is centrosymmetric. 2. the value is continuous except for the diagonal line. 3. θ_{GB} is zero when the two grains have symmetrical crystal orientation. Together with the criterion, selection maps are depicted and compared with CA and PF models [6] which show the significant differences in between. In this work, as the directional solidification experiments for Ti6Al4V under rapid solidification condition of MAM is still pending based on the knowledge of the authors, the selection map under a certain rapid solidification condition range in wire DED process is depicted from experimental data, and regression is achieved with the help of ANN (methodology can be found in [14]).

3. Model establishment

Based on the physical realities of solidification condition in MAM described above, an "invasion model" for Ti6Al4V is established in this work to simulate the solidification microstructure evolution in DED processes. Instead of chasing for methods to directly mimic the grain growth, the invasion model focuses on the interaction between the neighboring grains within bi-crystal systems under different local solidification conditions and quantitively analysis the grain boundary angles. Invasion model introduced an "invasion factor" to describe a transient grain boundary behavior between a bi-crystal, as the parameter angle is a non-dimensional number which can be easily adapted into models where multiple scales are involved. The competitive grain growth behavior of columnar grains in DED fabricated Ti6Al4V is considered as a sum-up of all the invasion behavior in bi-crystal systems. According to physical realities discussed in the previous sector, the grain boundary angle between two adjacent grains from the normal direction of the solidification front is a result of the Marangoni effect (θ_M) and grain selection (θ_c), and these two effects are considered to be independent of each other in the invasion model. Under different cooling conditions ($G\&R$), these two effects can be summed up for the competitive grain growth within a bi-crystal model. Regarding the normal direction of the solidification front, the transient grain boundary angle (θ_{GBt}) within a bi-crystal system under certain solidification condition is given by:

$$\theta_{GBt} = \theta_c + \theta_M \tag{4}$$

The solidification in MAM is highly non-equilibrium as it takes place in a rapid manner, and the solutes of alloy systems cannot fully defuse towards or away from the solidification front (solute trapping effect). Recent PF models have considered how to consistently and quantitatively integrate non-equilibrium effects [15], however, for extreme solidification conditions in MAM, it is still a difficulty in traditional solidification microstructure simulation methods. In this work, a data-driven method is chosen to describe the competitive grain growth behavior within bi-crystal systems under different rapid solidification conditions. Here, we considered a limited solidification condition range in the DED process with an imposed solidification rate of 0-50 mm/s and a thermal cooling rate of 10^3 - 10^4 k/s. The grain selection map is depicted with the help of the ANN model where the training data comes from the experiment matrix, additional details can be found in [14]. Then the generated dataset becomes one engine of a continuous solidification microstructure simulation to describe the anisotropic growth effect of the two grains in a bi-crystal system under different local solidification conditions.

Studies have shown that <001> texture can generate along the buildup direction after passing the initial tens layers of material deposition, the grain size inherited from substrate growth into a relatively stable level and "invasion model" can be applied into the columnar grain dominating areas where the constrained solidification condition is achieved. Within a timestep of invasion model, first, the investigated area is discrete into a regular lattice arrangement. Based on the transient melt pool geometry, the cells are divided into different types including fusion, mushy and solid cells. Then, the crystal orientation information on the bottom of the simulation domain is extracted from EBSD experimental result. As shown in Figure 2, the cells located on the grain boundary at the solidification front is recognized. Based on the position of the grain boundary cell, the solidification condition is extracted either from the experiment or the other transfer phenomenon simulation models. Finally, the grain boundary angle is calculated from the invasion model, and the tangent value of the grain boundary angle is set at the grain boundary cell (mushy cells located at grain boundary positions) to describe the transient grain boundary invasion behavior within a timestep.

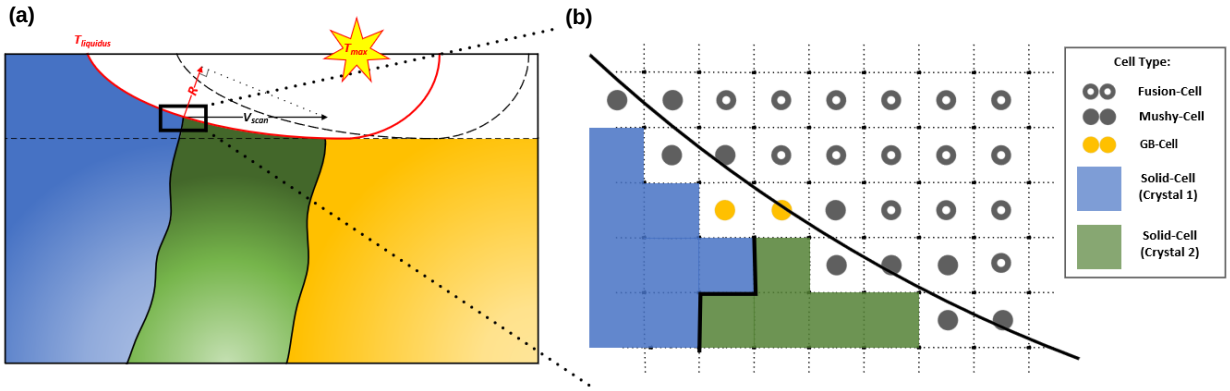

Figure 2: One timestep in the invasion model. a. Schematic of local solidification condition. b. Numerical representation of the simulation domain.

According to the simulation target and surrounding environment described above, the main assumptions adopted in this work include:

1. All the sub-grain microstructures and grain boundary migration are ignored

2. Melt pool geometry is considered relatively stable in each scanning pass and the fluctuation at the start and end position of the scanning track is ignored
3. No nucleation assumption with all epitaxial grain growth dominating the deposition process
4. Columnar grain size is much bigger than primary arm spacing
5. Solidification front can always catch up with the scanning speed of the DED process

Overall, the invasion model believes the tilt of grain boundary angles w.r.t the solid and liquid interface in the DED process is a sum-up of Marangoni and anisotropic growth effect. The important features are detailed in the following sections to describe the boundary condition, grain growth environment, and the grain boundary development.

3.1 Crystal orientations

For crystal orientations, columnar grains inherit the crystal information (including crystal orientation and size) from the previous layers of materials and nuclei on the existing half-melted crystals because of the epitaxial grain growth behavior. To achieve a quantitative microstructure simulation, an accurate boundary condition of crystal orientation and initial grain topological structure is the required. When the printed part has passed the initial several layers (5-10 layers) of competitive grain growth, a texture appears which decreases the intensity of grain competition, so the columnar grain size in the XY plane becomes relatively stable. In this case, the boundary condition is set based on crystal reconstruction result, and <001> directions reflection on the corresponding plate is used in 2D models. In real practice, the bottom area of printing is usually left for cutting or support structures making the microstructure inside less important. For the cases in which new crystals or nucleation are introduced in the process (SLM or laser powder DED), the boundary condition with random crystal orientations and grain structure using Voronoi diagram is acceptable because it is impossible to set the boundary condition based on experiment considering the complexity of the process.

3.2 Local Solidification Condition

In most of the MAM cases, the melt pool is generated by a high energy beam. As the MAM fabricated part is composed of a mass of welds, the microstructure in a single weld bead decides the final solidification microstructure of the fabricated part. The transient melt pool geometries are crucial and being the prerequisite to get an accurate simulation result. To capture the melt pool geometrical along the building process, a well-tested CFD model is used to reproduce transient the melt pool geometries with experimental validation. Details of the establishment of the CFD model can be found in [16]. The key attributes of the melt pool geometry can also be adopted from the finite element method (FEM) result or analytical solutions [17].

The melt pool geometry is considered as the isothermal surface along the liquidus line, closely attached to the mushy zone. It is a direct reflection of the local solidification conditions. The cooling condition along the melt pool bottom changes dramatically in terms of $G\&R$, and in turn, influences the solidification microstructure developed subsequently. To calculate the transient solidification condition for the bi-crystal systems, the attributes of a transient fusion zone including melt pool length (L_m), width (W_m), depth (D_m), and displacement (d_m) are extracted from the melt pool geometry of CFD simulation after experimental validation. Then, the “double ellipsoid approximation” is used to mathematically represent the transient melt pool geometry. To accurately capture the normal direction and solidification condition of a solidification front, the segment of an ellipsoid is carefully matched with the simulated fusion zone at the melt pool

tail. This ellipsoid can be defined by a simple equation (for thin-wall structure, the tilt of melt pool is ignored) where the original locates at the center of laser beam:

$$\frac{x^2}{{L_m}^2} + \frac{y^2}{{W_m}^2} + \frac{(z-d_m)^2}{(D_m+d_m)^2} = 1, \quad (z \le 0) \tag{5}$$

On the x-z plane locating at the center of the melt pool ($y=0$), we take the differential of Eq. (5) and obtain

$$\frac{dz}{dx} = -\frac{(D_m+d_m)^2}{{L_m}^2} * x, \qquad (z \le 0) \tag{6}$$

From the above mathematical model, solidification conditions in terms of $G\&R$ are calculated. In terms of the thermal gradient, the maximum heat flux direction can be captured from the normal direction of isotherm as the negative reciprocal value of dz/dx is the tangent value of the thermal gradient direction on the X-Z plane. The thermal gradient value can also be generally calculated as $(T_{max} - T_{liquidus})/\sqrt{x^2 + z^2}$. For the solidification rate, it is represented by

$$R = -\frac{{L_m}^2}{(D_m+d_m)^2} * \frac{(z-d_m)}{x} * v_{scan}, \quad (z \le 0) \tag{7}$$

The same principle can also be applied to Y-Z and X-Y planes. The grain boundary angle attributed by anisotropic growth effect under a local solidification condition is considered as a function of thermal gradient value, solidification rate, crystal orientations of the two grains in the bi-crystal system.

$$\theta_c = f(G, R, \alpha_1, \alpha_2) \tag{8}$$

As this function is highly nonlinear, in this work it is achieved by the regression of experimental data by ANN model with solidification condition and crystal orientations being the selected features. The methodology and details can be found in [14]. Under this strategy, the effect of grain boundary energy and force balance on grain boundary trijunctions [18] are implicitly included in the "invasion model" as they also can be considered as dependent features of the ANN model.

We now develop the theory a step further to consider the influence of the Marangoni effect on the grain boundary angle. Here, we assume there is perfect mixing in the liquid far from the solidification front because of the strong stirring effect and the alloy material add to the melt pool. Various simulation works have shown that the convection around a growing alloy crystal can influence the grain growth behavior dramatically [19]. Apparently, the stirring leads by the Marangoni effect change the concentration field near the solidification front and boundary layer thickness thus provides different constitutional supercooling which is the major contribution for alloy solidification.

Suggested by Papapetrou [20] that a parabolic isoconcentration interface geometry satisfies the shape-preserving condition as only a part of latent heat or solute is rejected ahead of growing dendrite to keep a constant dendritic tip grain growth velocity. For alloy solidification, the rest of the solute is dissipated along the sides which decreases the constitutional supercool and hinders the grain growth of secondary branches. Following this, the normal growth velocity approaches to zero for the secondary dendrites far from the tip. This leads to the invariant thermal and solute concentration field condition in the directional solidification problem so that a parabolic dendrite

can grow with a constant velocity (V). The invariant solute field can then be obtained for the steady-state diffusion equation with a moving coordinate system at the dendrite front:

$$\nabla^2 C + \left(\frac{V}{D}\right)\left(\frac{\partial C}{dz}\right) = 0 \quad (9)$$

With C stands for solute concentration, D is solute diffusion coefficient and z is the dendritic tip growth direction. The invasion model believes that the shape-preserving condition is rarely encountered in the practice of MAM, especially at the grain boundary area because of the asymmetrical solute concentration field lead by Marangoni convection. Inevitably, the stirring effect of the moving fusion tends to reduce the solute concentration on the side facing against the liquid flow direction and provide extra constitutional supercooling and grain growth environment for a continuous generation and growth of secondary dendrites (as shown in Figure 3), thus generates a horizontal grain growth velocity and influence the grain boundary angle.

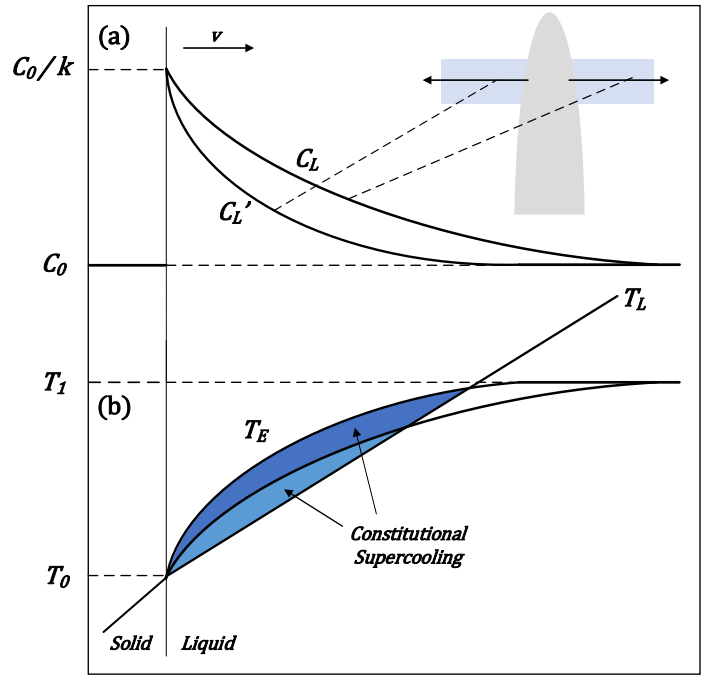

Figure 3: The origin of constitutional supercooling on both sides of dendrite under the Marangoni effect. a. Composition profile across solid/liquid interface with direction point away from the interface. b. The temperature profile (T_L) ahead of the interface with the difference between T_L and equilibrium liquidus temperature (T_E) representing the different constitutional supercooling on both sides. T_1 and T_0 stand for the equilibrium temperature of the solidus and liquidus line.

The growth velocity of these secondary dendritic tips (V_{tip}), with its reflection on solidification front referred as horizontal grain growth velocity (V_{GBh}), is adapted from the Kurz–Giovanola–Trived (KGT) model [21]. By using the solute supersaturation, Ω, as an intermediate variable under Ivantsov function of the solute Peclet number: $Iv(Pe)$, the relationship between dendrite tip growth rate and undercooling yields to

$$V_{tip}(\Delta T) = \frac{D_L}{5.51\pi^2(-m(1-k)^{1.5})\Gamma}\left(\frac{\Delta T^{2.5}}{{C_0}^{1.5}}\right) \quad (10)$$

where D_L is the solute diffusion coefficient in the liquid, m is the liquidus slope, k is the partition coefficient, Γ is the Gibbs-Thomson coefficient, C_0 is the initial concentration, detailed steps and derivation can be found in [4, 22]. Then the grain boundary angle attributed to Marangoni effect (θ_M) can be represented by

$$\theta_M = \tan^{-1}(V_{GBh}(\Delta T)/R) \quad (11)$$

Under the assumption that melt pool geometry is relatively constant within a single scan, the grain boundaries in each layer experienced similar solidification conditions from the bottom of the melt pool to its top in the x-z plane. Thus, the influence of Marangoni effect on grain boundary angles within a hole layer thickness can be taken as a general integral average value and subtracted from the total grain boundary angle when considering the anisotropic growth effect.

3.3 Grain Boundary Invasion

In each timestep of solidification microstructure simulation, the local solidification condition between the melt pool tails area is considered as constant, and the transient grain boundary is presented as a straight line. To accurately depict the grain boundary angle in a spatially discretized numerical model, the length of the meshing grid is decided based on the dimension of the simulation target. In the case of the wire DED fabricated Ti6Al4V, as the columnar grain size can achieve several millimeters (characteristics feature size) and the layer thickness is around 0.7 mm, the cell size is set as 20 μm which is 35 times smaller than layer thickness to guarantee the simulation resolution.

This model is robust because an angle is a dimensionless number, and the angles representing anisotropic growth and Marangoni effects can be summed up without considering the magnitude of the discretized cells. After the grain boundary angle is calculated based on the above methodology at grain boundary positions, the grain boundary invasion behavior in a numerical model becomes simple. Here we define the invasion factor (IF) of a grain boundary within a bi-crystal system as:

$$IF = tan\ (\theta_{GBt}) \quad (12)$$

Under the cartesian coordinate system follows the convention of additive, the angle between a transient thermal gradient direction and build up direction in a 2D model is defined as θ_T and invasion factor becomes:

$$IF^{AM} = tan\ (\theta_{GBt} + \theta_T) \quad (13)$$

The invasion factor is then assigned at a single track of cells straightly above the grain boundary cell and accumulates the value from bottom to top in each timestep. Once a positive integer is reached, the cells (based upon the integer value) at the left of the straight grain boundary line are changed into the grain index on the right, and vice versa. To avoid network dependence and converge the simulation result, the timestep length is determined based on trial and error to accurately represent the grain boundary curve and at the meantime guarantee the efficiency.

Altogether the invasion model considers the competitive grain growth behavior in MAM as a summary of the grain boundary tilting among the adjacent crystals. The grain boundary angle is considered as a grain invading into its neighbor grains under the absolute coordinate system and changes the grain size, hence the "invasion model". This grain boundary angle w.r.t. the thermal

gradient direction under a local solidification condition is caused by anisotropic growth and the Marangoni effect. In the numerical application of the invasion model, an invasion factor is introduced to represent the tilting of transient grain boundary angles. In the following section, wire DED fabricated thin-wall structure is used to validate the invasion model.

4. Experimental Validation

The building configuration wire DED process is shown in Figure 4a. The samples were fabricated using a LAWS 1000 automated welding system equipped with a 1 kW YAG solid fiber laser. The deposition with Ti6Al4V ELI wire feedstock was operated under an Argon gas protection environment. The process parameters are shown in Table 1. The case of wire DED fabricated Ti6Al4V is selected as a benchmark for this study because the epitaxial grain growth eliminates most of the random factors of nucleation. On the other hand, the thin wall structure fabricated is a good example for a pseudo-3D case simulation model as the columnar grains are able to develop extremely big into millimeter level, where the grain size exceeds the thickness of the thin wall and thus guarantee there is only one grain in the whole thickness direction. This eliminates the influences caused by the grains coming from the side and focus on the competitive grain growth behavior of a set of columnar grains. A comparison with the powder DED process is provided in Figure 4b, half-melt powders are found at the surface of the fabricated part (Figure 4d). These half-melted powders inevitably provide epitaxial growth positions introducing extra crystals and influence the microstructure in the investigated domain. On the contrary, the wire DED process is capable to fabricate an accurate thin-wall structure with a clean surface on the side (Figure 4c), this indicates that melt pool geometry is relatively stable, and all the material experienced a melting and solidification process and eventually becomes the solidification microstructure in the fabricated part. To set up the boundary conditions based on the real experimental result and compare the simulation result with experiments, the following experimental activities are launched.

Table 1. Process parameters of the wire DED fabricated Ti6Al4V

Process Parameter	Heat source power (W)	Scanning Speed (mm/min)	Feed rate (mm/min)
Wire DED	625	431.8	889

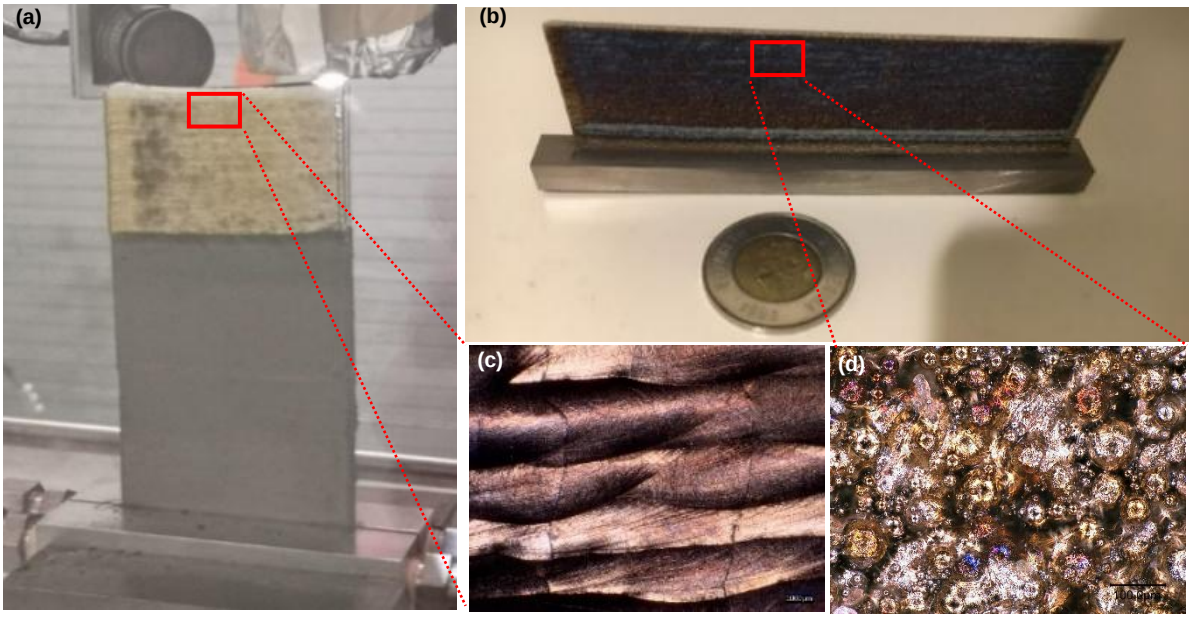

Figure 4: Building configuration and surface topology comparison of the wire (a, c) & powder (b, d) DED fabricated Ti-6Al-4V thin wall structures

4.1 Characterizations of microstructures

As can be seen from Figure 5a, the microstructure of wire DED fabricated Ti6Al4V at room temperature shows a full basketweave structure (α). In some cases of the DED process with good cooling conditions, a full martensite structure (α') can be achieved. The solid phase transformation of Ti6Al4V eliminates most of the original crystal (prior β) information with primary and higher-order branches of the same column grain merged with each other. The crystal orientation information can be captured from EBSD reconstruction techniques [23] as the solid phase transformation of Ti6Al4V strictly follows the Burgers orientation relationship (BOR). Along the buildup direction, EBSD is carried out in three separate areas of each column grain for the reconstruction (Figure 5b). Maps of three Euler angle is shown in Figure 5c and the misorientation of reconstruction result is lower than two degrees. This small misorientation can be attributed to the crystal deformation lead by the high residual stress generated during the printing process. Also, the accuracy of the EBSD technique to distinguish a different crystal orientation is typically around 0.5 degrees, so the accuracy of the EBSD reconstruction technique is believed to be satisfied. However, the EBSD technique usually limits the size of the testing sample and it is time and cost consumable. Thus, it is only used to capture the crystal orientation information of the solidification microstructure, and the grain topological structure reconstruction method in a part level is presented in the following section by extracting the grain boundaries of the column grains from sample surface and cross-sections.

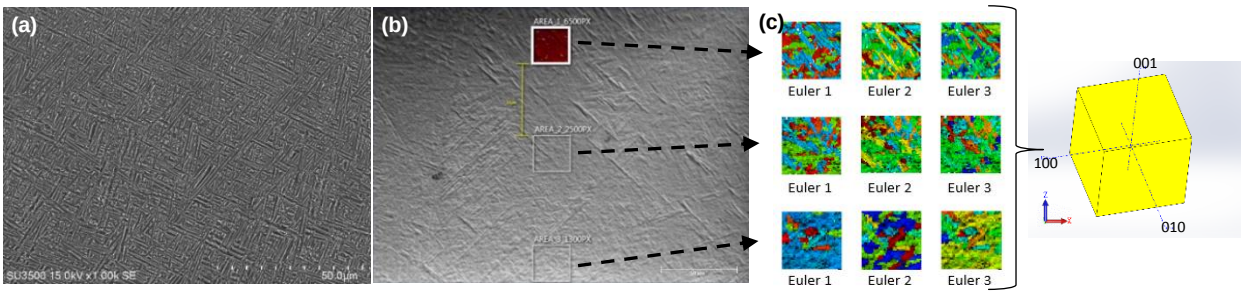

Figure 5: Microstructure of wire DED fabricated Ti6Al4V thin-wall structure. a. Electron microscope of the basketweave structure (fully α' phase). b. Three detected areas (spaced at 50μm) within the same prior β grain. c. The three corresponding Euler angle maps of α' grain and the reconstructed crystal orientation present of the prior β grain.

4.2 Grain boundary extraction & grain topological structure reconstruction

For the grain topological structure, the columnar grain morphologies cannot be reconstructed under a high amplification observation condition because of the solid phase transformation and the scale limitation. Luckily, different prior β grains with different crystal orientations have different absorbance abilities of the visible light and we can recognize them with an optical microscope, distinguishing columnar grains with different crystal orientations is more obvious after chemical etching which can be observed with naked eyes. Moreover, the grain boundaries are areas filled with defects, for as the concentration of the dislocation in the low-angle tilt boundaries. These defects on the grain boundaries will also lead to different resistance to etchant and a contract between their neighboring grains. On the surface of the printed part, grain boundaries also have a clear groove as they are the last solidified area compared to the inner area of grain, as shown in Figure 6a. The grain size and grain boundaries are extracted from the imaging results in a part scale under the help of image segmentation software (Figure 6b achieved by Dragonfly). For a 3D reconstruction of the grain topological structure, the thin-wall samples are cut from the center on the X-Z plane and the above methods are used comprehensively to achieve a grain structure reconstruction on a large scale.

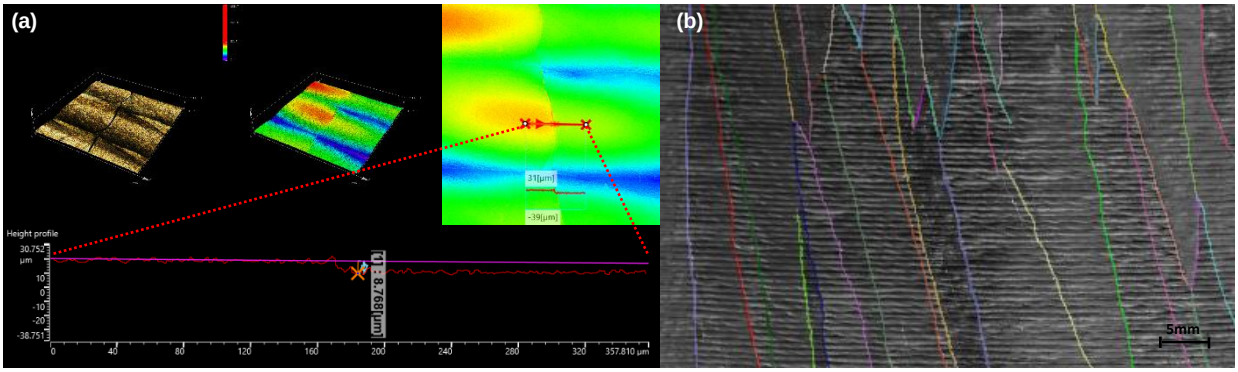

Figure 6: Laser confocal imaging of the grain boundary area. a. 3D optical image and contour map with the extracted cross-section height profile of grain boundary area. b. Grain boundary recognition under image segmentation.

4.3 Transient Melt Pool Geometry Attributes

We can never overestimate the importance of melt pool geometry to the resultant solidification microstructure in MAM. All solidification microstructure simulation works in part scale should carefully validate the melt pool geometry during the printing process to provide accurate solidification condition and boundary condition for the simulation domain. In Figure 7a, a high-speed camera focusing on the melt pool domain is used for melt pool geometry validation. From the captured images and laser center position, the length and width of the fusion zone are measured. The depth of the melt pool and overlap between layers are be measured from Y-Z cross-sections of the samples after chemical etching. The comparison between CFD simulation (Figure 7b) and experiment (both under single-track multi-layer configuration) is shown in Figure 7a where the melt pool geometry of the simulation coincides with experimental observation. For a more accurate melt pool geometry, the current research on the ultrahigh-speed synchrotron X-ray imaging could provide more insights [24].

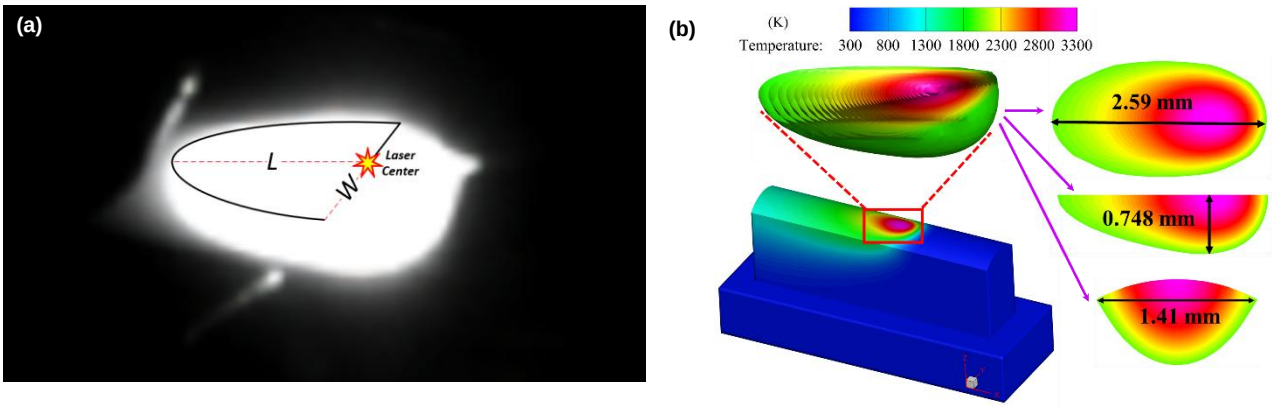

Figure 7: Melt pool geometry validation. a. High-speed imaging of transient melt pool geometry with L and W representing the length and width of the melt pool. b. Melt pool geometry extracted from the CFD simulation.

5. Results and discussion

The invasion model is carried out in a pseudo-3D case of a thin wall structure with a dimension of 22*2.6*7 mm^3 (10 layers). The solidification microstructure of the material deposited is simulated with a layer overlap of 38%. To keep the "relatively stable melt pool geometry" assumption valid, the simulation domain (shown in Figure 8a) is selected in the center (scanning direction) area of a thin wall to avoid melt pool geometry fluctuation and the printed part distortion located at both ends of a scanning track. For a quantitative comparison between the simulation and experimental result, the simulation domain also locates at the top of the printed part where the initial competitive grain growth inherits from the substrate is finished, and the columnar grains exceed the thickness of the thin wall eliminating the influence of the grains coming from the side.

Based on the integrated application of reconstruction techniques introduced in the experimental validation section, the image segmentation of different grains (Figure 8b) and the 3D reconstruction of grain geometrical structure (Figure 8c) in the target domain are achieved. The boundary condition of crystal orientation and initial grain structure are set directly based on the experimental result. After the initial several layers of material deposition, strong texture starts to

emerge with <001> directions of the crystal generally parallel with the buildup direction. In this pseudo-3D model (a combination of multiple X-Z layers), the reflection of [001] direction of the crystals is used to represent the crystal orientations in the 2D cases.

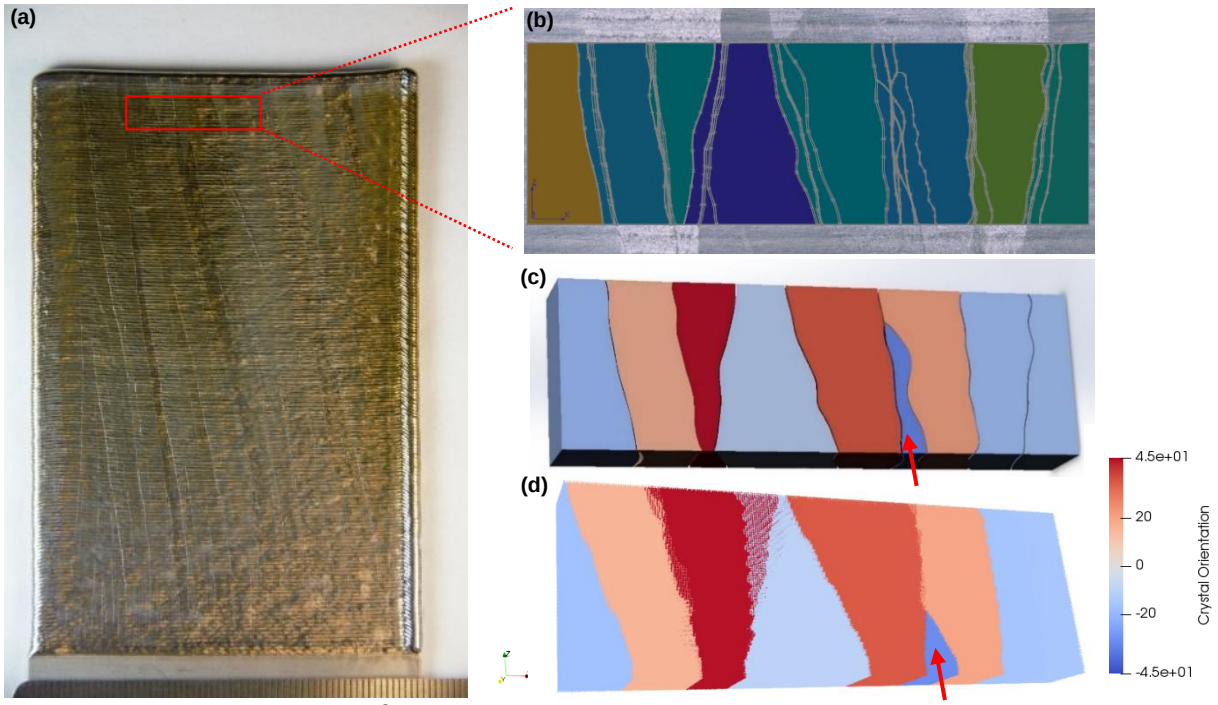

Figure 8: The application of the invasion model on the thin-wall structure. a. The simulation domain on a wire DED fabricated thin-wall structure. b. Grain boundary extraction on the three corresponding layers. c. Grain structure reconstruction result. d. Simulation result of the invasion model.

This invasion model was launched under a self-developed *C++* environment and the simulation result is visualized by a data visualization software (*ParaView*). Under the 8 core CPU processor (Intel (R) Core (TM) i5-10300H), it took only 12 minutes to achieve the above simulation with a cell size of 20 µm. The simulation result of the solidification microstructure is shown in figure 8d which has a perfect match with the experimental result showing the increase and decrease of grain size along the material deposition process. It is also worth noting that the model accurately predicts the failure of the grain (highlighted in Figure 8c&d) during the competitive grain growth. This also indicates the application potential of the invasion model in other grain selection studies. The average grain size change of grain geometrical reconstruction and simulation along the material deposition process in different layers is shown in Figure 9. The average grain size shows a perfect match between simulation and experimental reconstruction results in the first four and last two layers. However, vigorous increases are found at layer five and eight in simulation and experiment, respectively. This can be mainly attributed to the grain eliminating at the corresponding layer, and the invasion model can rapidly recover its simulation accuracy within a short length range.

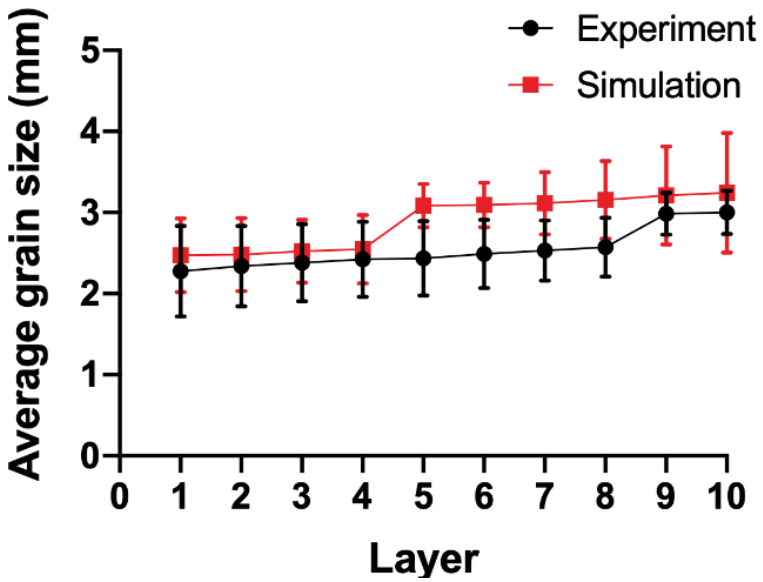

Figure 9: Average grain size comparison between experimental and simulation results.

For complex cases like solidification microstructure in MAM, the authors believe there is no short path as many in-process parameters are not being quantified. In this simulation framework, we take as much experimental data as input as possible and solve this problem by building up databases, and other simulation models are used to fill the gap where experimental data is hard to get. A careful selection and coupling of various models with the appropriate application range is the only way to achieve an accurate, long scale simulation with practical efficiency. The proposed invasion model is designed for constrained columnar grain growth like most cases in MAM when equiaxial grains are hard to achieve. However, the application field is not suitable for equiaxial grain growth with homogeneous nucleation in liquid as the invasion model cannot accurately track the grain boundary before the adjacent grains get in touch. The traditional methods such as the grain tip kinetic (CA) and deriving the field form (PF) are still very useful for the equiaxial grain growth and the invasion model can be a good complement when the prerequisite conditions are achieved.

The framework developed in this work also shows its practical importance when the solidification conditions are extreme and the traditional solidification theory being invalid. This strategy of the invasion model is robust, and it can be applied to achieve an accurate solidification microstructure simulation for other types of material where current simulation methods are not suitable. It can also be coupled with other macroscale models or introduce data from models. When the invasion model is applied, the real problem becomes how to get the accurate local solidification condition, boundary condition and nucleation rules set up. In-situ characterization is a good way to provide accurate transient melt pool information [24], and the invasion model can be combined with the real-time experimental monitoring techniques to achieve a more accurate simulation result.

6. Conclusions

As many probabilistic models of solidification microstructure simulation are having difficulties when dealing with MAM processes, a deterministic model (named invasion model) is developed

in this work to provide a quantitative prediction of solidification microstructure. With the wire DED process as a benchmark, the invasion model focuses on the grain boundary development within bi-crystal systems, and it believes the competitive grain growth behavior is a sum-up of all the invasion behavior of bi-crystal systems. By analyzing the effect of Marangoni and anisotropic growth, the transient grain boundary angles of columnar grains are represented by an invasion factor in the numerical model. To the best of the authors' knowledge, the grain boundary angles of MAM fabricated Ti6Al4V is never quantitatively studied before this work. Also, the invasion model provides a methodology to investigate the solidification microstructure for most of the alloy systems under a rapid solidification condition which is now still a difficulty for existing methods. When the traditional solidification theory frequently lost its efficacy on the simulation work (especially on the topics of nucleation), we realize that the establishment of databases for the key sub-processes is also important for a more accurate simulation. On the other hand, the invasion model is very practical as it can quantitively depict the grain structure of columnar grains in a part scale with high accuracy and computational efficiency. The strategy is robust which can be combined with various existing mechanistic models. By combining with real-time monitoring data, we believe this model can be a good tool for process optimization in MAM and push the microstructural control into the next level of accuracy.

Acknowledgment

This research was supported by the Natural Sciences and Engineering Research Council of Canada (NSERC) Collaborative Research and Development Grant CRDPJ 479630-15. The lead author also received partial funding from the NSERC Collaborative Research, Training Experience (CREATE) Program Grant 449343, and the National Key Research and Development Program of China (Grant No. 2018YFB0703400). We acknowledge Dr. Zhibo Luo and Ms. Yuan Yao for the discussion and help during sample characterization. The lead author would also like to thank McGill Engineering Doctoral Award (MEDA) grant and China Scholarship Council (201706460027).

Reference

[1] T. Keller, G. Lindwall, S. Ghosh, L. Ma, B.M. Lane, F. Zhang, U.R. Kattner, E.A. Lass, J.C. Heigel, Y. Idell, Application of finite element, phase-field, and CALPHAD-based methods to additive manufacturing of Ni-based superalloys, Acta materialia 139 (2017) 244-253.

[2] K. Karayagiz, L. Johnson, R. Seede, V. Attari, B. Zhang, X. Huang, S. Ghosh, T. Duong, I. Karaman, A. Elwany, Finite interface dissipation phase field modeling of Ni–Nb under additive manufacturing conditions, Acta Materialia 185 (2020) 320-339.

[3] S. Ghosh, K. McReynolds, J.E. Guyer, D. Banerjee, Simulation of temperature, stress and microstructure fields during laser deposition of Ti–6Al–4V, Modelling and simulation in materials science and engineering 26(7) (2018) 075005.

[4] J. Li, X. Zhou, M. Brochu, N. Provatas, Y.F. Zhao, Solidification Microstructure Simulation of Ti-6Al-4V in Metal Additive Manufacturing: A Review, Additive Manufacturing (2019) 100989.

[5] J. Liu, A.C. To, Quantitative texture prediction of epitaxial columnar grains in additive manufacturing using selective laser melting, Additive Manufacturing 16 (2017) 58-64.

[6] A. Pineau, G. Guillemot, D. Tourret, A. Karma, C.-A. Gandin, Growth competition between columnar dendritic grains–Cellular automaton versus phase field modeling, Acta Materialia 155 (2018) 286-301.
[7] S. Kumar, W.A. Curtin, Crack interaction with microstructure, Materials today 10(9) (2007) 34-44.
[8] S. Kou, Welding metallurgy, New Jersey, USA (2003) 431-446.
[9] D. Tourret, Y. Song, A.J. Clarke, A. Karma, Grain growth competition during thin-sample directional solidification of dendritic microstructures: A phase-field study, Acta Materialia 122 (2017) 220-235.
[10] A. Wagner, B. Shollock, M. McLean, Grain structure development in directional solidification of nickel-base superalloys, Materials Science and Engineering: A 374(1-2) (2004) 270-279.
[11] J.H. Martin, B.D. Yahata, J.M. Hundley, J.A. Mayer, T.A. Schaedler, T.M. Pollock, 3D printing of high-strength aluminium alloys, Nature 549(7672) (2017) 365.
[12] D. Zhang, D. Qiu, M.A. Gibson, Y. Zheng, H.L. Fraser, D.H. StJohn, M.A. Easton, Additive manufacturing of ultrafine-grained high-strength titanium alloys, Nature 576(7785) (2019) 91-95.
[13] D. Walton, u.B. Chalmers, The origin of the preferred orientation in the columnar zone of ingots, Transactions of the American Institute of Mining and Metallurgical Engineers 215(3) (1959) 447-457.
[14] J. Li, M. Sage, X. Guan, M. Brochu, Y.F. Zhao, Machine Learning-Enabled Competitive Grain Growth Behavior Study in Directed Energy Deposition Fabricated Ti6Al4V, JOM 72(1) (2020) 458-464.
[15] T. Pinomaa, N. Provatas, Quantitative phase field modeling of solute trapping and continuous growth kinetics in quasi-rapid solidification, Acta Materialia 168 (2019) 167-177.
[16] Q. Meng, X. Zhou, J. Li, Z. Cui, Y. Wang, H. Zhang, Z. Li, C. Qiu, High-throughput laser fabrication of Ti-6Al-4V alloy: Part I. Numerical investigation of dynamic behavior in molten Pool, Journal of Manufacturing Processes 59 (2020) 509-522.
[17] M.N. Ahsan, A.J. Pinkerton, An analytical–numerical model of laser direct metal deposition track and microstructure formation, Modelling and Simulation in Materials Science and Engineering 19(5) (2011) 055003.
[18] S. Ghosh, A. Karma, M. Plapp, S. Akamatsu, S. Bottin-Rousseau, G. Faivre, Influence of morphological instability on grain boundary trajectory during directional solidification, Acta Materialia 175 (2019) 214-221.
[19] H. Wei, G. Knapp, T. Mukherjee, T. DebRoy, Three-dimensional grain growth during multi-layer printing of a nickel-based alloy Inconel 718, Additive Manufacturing 25 (2019) 448-459.
[20] A. Papapetrou, Untersuchungen über dendritisches Wachstum von Kristallen, Zeitschrift für Kristallographie-Crystalline Materials 92(1-6) (1935) 89-130.
[21] W. Kurz, B. Giovanola, R. Trivedi, Theory of microstructural development during rapid solidification, Acta Metallurgica 34(5) (1986) 823-830.
[22] D.C. Tsai, W.S. Hwang, A three dimensional cellular automaton model for the prediction of solidification morphologies of brass alloy by horizontal continuous casting and its experimental verification, Materials transactions 52(4) (2011) 787-794.
[23] C. Cayron, B. Artaud, L. Briottet, Reconstruction of parent grains from EBSD data, Materials Characterization 57(4-5) (2006) 386-401.
[24] R. Cunningham, C. Zhao, N. Parab, C. Kantzos, J. Pauza, K. Fezzaa, T. Sun, A.D. Rollett, Keyhole threshold and morphology in laser melting revealed by ultrahigh-speed x-ray imaging, Science 363(6429) (2019) 849-852.